International Journal of Solids and Structures 47 (2010) 887–893

Contents lists available at ScienceDirect

International Journal of Solids and Structures

journal homepage: www.elsevier.com/locate/ijsolstr

On the most dangerous V-notch

A. Carpinteri, P. Cornetti *, N. Pugno, A. Sapora

Department of Structural Engineering and Geotechnics, Politecnico di Torino, Torino, Italy

ARTICLE INFO

Article history:
Received 27 June 2009
Received in revised form 26 October 2009
Available online 27 November 2009

Keywords:
V-notches
Notch sensitivity
Brittleness number
Finite fracture mechanics

ABSTRACT

The determination of the failure load for brittle or quasi-brittle specimens containing a re-entrant corner has been faced by several authors, whose approaches are available in the Scientific Literature. However, up to now, little attention has been paid to the presence of a minimum, i.e. an angle at which the critical load attains its minimum value. Even if the minimum was detected in several experiments, it was not highlighted or it was considered as a mere consequence of the scattering of experimental data. Restricting the analysis to a sharp V-notched infinite slab under a remote tensile load, the problem is fully investigated in this paper. It is shown that a minimum, more or less pronounced according to the brittleness number, is always present. It means that the edge crack is not the most dangerous configuration, although the notch opening angle providing the minimum failure load tends to vanish for large notch depths as well as for very brittle materials.

© 2009 Elsevier Ltd. All rights reserved.

1. Introduction

Aim of the present paper is to provide an answer to the following question: is the edge crack the most dangerous V-notch? Although when machining a V-notch from a plain specimen, the larger the notch amplitude, the larger is the amount of removed material, within a brittle structural behaviour it is reasonable to expect a lower failure load for a vanishing notch opening angle, since an higher order singularity occurs in the stress field at the tip for the edge-cracked geometry.

However, looking at the experimental data on sharp V-notched specimens available in the literature, it is seen that, for a remarkable number of tests, the failure load does not increase monotonically as the notch opening angle ω increases. In other words, it seems to exist a critical angle ω_c for which the failure load attains the minimum value.

Let us consider more in detail the experimental data. Carpinteri (1987) tested three point bending (TPB) PMMA specimens with a V-notch opening angle ω equal to 0°, 45°, 90°, 120°, 150°, 180°. He performed two series of tests, with a relative notch depth equal to 0.2 and to 0.4 respectively; each geometry was tested three times. For both the series the minimum failure load was exhibited by the 45° specimen. It is worth noticing that, with respect to the other geometries, a larger scatter in the failure loads values was observed for the cracked ($\omega = 0°$) specimens; furthermore, note that the cracks were obtained by narrow sawed slits.

Seweryn (1994) tested double edge notched PMMA specimens under tensile load. The notch opening angle was chosen every 20° in the range 20°–180°. Also in this case, each geometry was tested three times. The geometry providing the minimum critical load was the 40° sample.

Strandberg (2002) tested single edge notched tensile specimen. The material was a soft annealed tool steel tested at – 50°C to enhance the tendency for a brittle fracture. The notch opening angle ω was taken equal to 0°, 30°, 60°, 90°, 120°, 140°. Each geometry was tested three times. The cracked specimens are the ones providing the minimum failure load. However, while the notches were machined, the cracked geometry was manufactured by first pre-cracking an ordinary TPB specimen to the desired crack depth. As stated by the Author himself, the lower values obtained for the cracked specimen is probably due to the difference in acuity between a fatigue crack and a machined notch and to the weakening effect of the pre-cracking procedure. On the other hand, by passing from 30° to 60°, the failure load slightly decreases. Afterwards it increases monotonically with ω, so that 60° can be regarded as a (relative) minimum.

Gómez and Elices (2003) tested PMMA TPB samples with a V-notch opening angle ω equal to 0°, 15°, 30°, 60°, 90°, 120° and 150°. The notched samples were obtained by a low-speed cutter whereas the crack in the pre-cracked specimens was obtained by an incision with a razor blade. A minimum of four specimens were tested for each configuration. In this series of test, the failure loads show an oscillating trend between 0° and 90°, with two local minima for 15° and 60°, followed by the usual ascending branch after 90°.

Other tests on sharp V-notched specimens were performed by Grenestedt et al. (1996), by Dunn et al. (1997) and by Carpinteri et al. (2009), who tested expanded PVC foam, PMMA and polystyrene specimens respectively. In such tests, the failure loads were always increasing with the notch angle, but they are of little help

* Corresponding author.
E-mail address: pietro.cornetti@polito.it (P. Cornetti).

0020-7683/$ - see front matter © 2009 Elsevier Ltd. All rights reserved.
doi:10.1016/j.ijsolstr.2009.11.017

to decide whether a minimum is present or not, since only one or no one geometry was tested in the range 0°–90°. However, it is worth observing that almost the same failure load was recorded (Carpinteri et al., 2009) for the polystyrene specimens of the 60° and 120° geometries (polystyrene being a relatively ductile material).

Note that all the cited tests were aiming to analyze sharp V-notches, so that the notch root radius was kept as small as possible. Of course, the presence of a finite notch root radius increases the strength of the V-notched specimen: namely, the more brittle is the material, the larger is the strength increment. Strandberg (2002) and Gómez and Elices (2003) provided also some theoretical predictions to take into account the notch blunting effect.

Aim of the present paper is not to provide a theoretical prediction for all the aforementioned tests. Since, from experiments, the presence of a minimum failure load seems to be a general feature independently of the material, geometry and loading type, for the sake of generality in the present analysis we will deal with the ideal case of a semi-infinite sharp V-notched slab under a remote tensile load (Fig. 1a), when the notch is subjected to mode I loading.

Note that some theoretical predictions showing the presence of the minimum for specific finite size geometries are already available in the literature (Lazzarin and Zambardi, 2001; Carpinteri et al., 2008, 2009). Other predictions will be the subject of forthcoming studies.

2. Semi-infinite V-notched plate under uniaxial remote tension

The stress field solution near the vertex of a re-entrant corner of amplitude ω in a linear elastic plate was addressed by Williams in his pioneering work (Williams, 1952). In the case of mode I loading, his solution shows that the stresses at the vertex of the re-entrant corner are unbounded for any ω comprised between 0° and 180°. The stress singularity is of order $1-\lambda$, where $\lambda(\omega)$ is the solution of the eigen equation derived by Williams (1952) and is comprised between 1/2 ($\omega = 0°$) and 1 ($\omega = 180°$). In formulae:

$$\sigma_y(x) \cong K_I^*/(2\pi x)^{1-\lambda}, \quad x \to 0^+ \tag{1}$$

where x is the V-notch bisector and σ_y is the normal stress directed along y (see Fig. 1). K_I^* is the generalized stress intensity factor (sometimes referred to as notch-SIF), whose value depends on geometry and loading far from the notch. Restricting the analysis to a semi-infinite notched plate under remote tensile stress σ (Fig. 1a), dimensional analysis arguments yield the following expression for the generalized SIF (Carpinteri, 1987):

$$K_I^* = \beta(\omega)\sigma e^{1-\lambda} \tag{2}$$

where e is the notch depth and β is a dimensionless coefficient depending on the notch angle ω, whose tabulated values can be found in (Dunn et al., 1997). It varies from $1.12\sqrt{\pi}$ ($\omega = 0°$), when Eq. (2) coincides with the well-known formula for the SIF of an edge crack, to 1 ($\omega = 180°$), when the stress singularity disappears and Eq. (2) simply states that the generalized SIF coincides with the remote tensile stress.

The generalized SIF K_I^* is the coefficient of the dominant term in the stress field at the notch tip and, within brittle structural behaviour and sharp geometry, it is expected to be the governing failure parameter. In other words, failure is supposed to take place whenever (Carpinteri, 1987):

$$K_I^* = K_{Ic}^* \tag{3}$$

K_{Ic}^* being the generalized fracture toughness. Several approaches (Sih and Ho, 1991; Seweryn, 1994; Lazzarin and Zambardi, 2001; Leguillon, 2002; Gómez and Elices, 2003; Carpinteri and Pugno, 2005; Carpinteri et al., 2008) have been proposed in the literature to relate the generalized fracture toughness to the tensile strength σ_u and to the fracture toughness K_{Ic} of the material. All of them may be cast in the following expression:

$$K_{Ic}^* = \xi(\omega)\frac{K_{Ic}^{2(1-\lambda)}}{\sigma_u^{1-2\lambda}} \tag{4}$$

where ξ is a dimensionless coefficient depending on the notch angle ω. It is equal to 1 for 0° and 180°-notch amplitudes, when the generalized fracture toughness is equal to K_{Ic} and σ_u, respectively.

Note that, while the fracture toughness has to be obtained by testing cracked specimens according to standard recommendations, testing plain specimens to determine the material tensile strength could be not the best choice. In fact, if the material is not ideally brittle, un-notched specimens may exhibit a non-linear behaviour, whereas the behaviour of notched specimens remains linear. Under these circumstances, in Eq. (4), σ_u should represent the maximum normal stress at incipient failure when testing, e.g., specimens with semicircular notches (Seweryn, 1994; Lazzarin et al., 2009). However, for the sake of simplicity, in what follows, we will refer to σ_u as the material tensile strength.

Eq. (4) was first set by Seweryn (1994), who, applying the average stress criterion, proposed $\xi = \lambda 4^{1-\lambda}$. However, a physically more convincing derivation of Eq. (4) may be obtained according to the coupled finite fracture mechanics (FFM) criterion (Leguillon, 2002; Cornetti et al., 2006). In order to apply FFM, the SIF for a short crack of length a at the V-notch root (and directed along the notch bisector) is needed:

$$K_I = \mu(\omega)K_I^* a^{\lambda-1/2} \tag{5}$$

Eq. (5) dates back to Hasebe and Iida (1978); μ is a dimensionless coefficient depending on the notch angle ω. Accurate μ values can be found in tabulated form in (Philipps et al., 2008; Livieri and Tovo, 2009). It increases from unity, when $\omega = 0°$, up to $1.12\sqrt{\pi}$, when Eq. (5) coincides with the well-known formula for the SIF of an edge crack ($\omega = 180°$).

The coupled FFM criterion is based on the hypothesis of a finite crack advancement Δ and assumes a contemporaneous fulfilment of stress equivalence (in critical conditions) and energy balance for crack propagation (Cornetti et al., 2006):

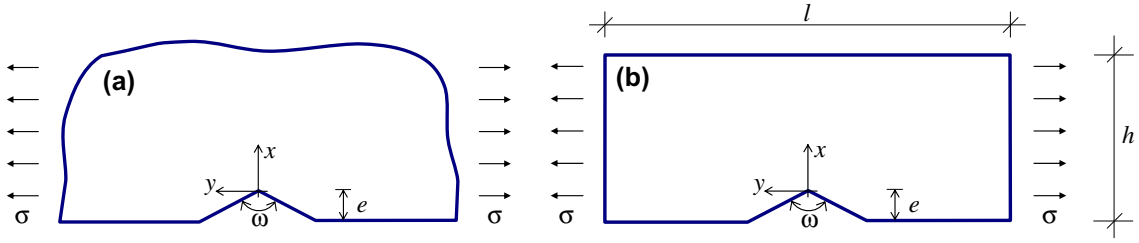

Fig. 1. Semi-infinite (a) and finite-size (b) V-notched plate under uniaxial remote tension.

$$\begin{cases} \int_0^{\Delta} \sigma_y(x)\,dx \geqslant \sigma_u \Delta \\ \int_0^{\Delta} K_I^2(a)\,da \geqslant K_{Ic}^2 \Delta \end{cases} \tag{6}$$

The former inequality requires that the average stress upon the crack advancement Δ is higher than the material tensile strength; the latter one ensures that the energy available for a crack increment Δ is higher than the energy necessary to create the new fracture surface. It can be proved that the failure load (i.e. the lowest load satisfying Eq. (6)) is attained when the inequalities are strictly verified, i.e. they are replaced by two equations. In such a case Eq. (6) becomes a system of two equations in two unknowns, the crack advancement Δ and the failure load, i.e. the critical value K_{Ic}^* of the generalized SIF K_I^*. Upon substitution of Eqs. (1) and (5) into the system (6), Eq. (4) is recovered along with the following expression for the coefficient ξ:

$$\xi = \lambda^{\lambda} \left[\frac{(2\pi)^{2\lambda-1}}{\mu^2/2} \right]^{1-\lambda} \tag{7}$$

Furthermore, the crack advancement is equal to:

$$\Delta = \frac{2}{\lambda \mu^2 (2\pi)^{2(1-\lambda)}} \left(\frac{K_{Ic}}{\sigma_u} \right)^2 \tag{8}$$

The dimensionless coefficients λ, β, μ and ξ (according to Eq. (7)) are plotted vs. ω in Fig. 2 by means of a cubic spline interpolation of the values reported in Table 1. Note that, with respect to the expressions of ξ and Δ obtained in (Carpinteri et al., 2008), Eqs. (7) and (8) are more precise since the values of the coefficient μ used here are more accurate than the ones derived in (Carpinteri et al., 2008) by exploiting a superposition of the effects procedure along with suitable shape functions from SIF handbooks.

Inserting now Eqs. (2) and (4) into Eq. (3), yields:

$$\frac{\sigma_f}{\sigma_u} = \frac{\xi}{\beta} \alpha^{\lambda-1} \tag{9}$$

where σ_f is the remote tensile stress at failure and $\alpha = e \times (\sigma_u/K_{Ic})^2$ is the dimensionless notch depth.

Table 1
λ-, β-, μ- and ξ-values vs. notch opening angle ω. Note that the values of β and μ differ from the ones in (Dunn et al., 1997; Philipps et al., 2008) because of the different formal definition of generalized SIF K_I^* (Eq. (1)).

ω (°)	λ	β (from (Dunn et al., 1997))	μ (from (Philipps et al., 2008))	ξ (from Eq. (7))
0	0.5000	1.985	1.000	1.0000
30	0.5015	2.001	1.005	0.9968
60	0.5122	2.057	1.017	1.0004
90	0.5445	2.137	1.059	1.0071
120	0.6157	2.172	1.161	1.0168
150	0.7520	1.952	1.394	1.0226
180	1.0000	1.000	1.985	1.0000

Let us now recall the definition of the brittleness number $s = K_{Ic}/(\sigma_u \sqrt{e})$; s is a non-dimensional quantity, introduced by Carpinteri (1981a,b, 1982). Brittle structural behaviours are generally expected for low brittleness numbers. Note that in the present case, i.e. infinite slab, the characteristic structural size corresponds to the notch depth e, the only relevant size in the problem. Since $\alpha = 1/s^2$, Eq. (9) can be rewritten equivalently as:

$$\frac{\sigma_f}{\sigma_u} = \frac{\xi}{\beta} s^{2(1-\lambda)} \tag{10}$$

Hence the relative failure stress depends only on the notch amplitude through λ, β, ξ and on the material and notch depth through s.

Before proceeding, it is worth observing that, according to the coupled FFM criterion, the crack propagation from a V-notch is unstable if load controlled. FFM assumes a finite extension Δ at crack initiation; the subsequent crack propagation is ruled by classical linear elastic fracture mechanics (LEFM). In the geometry considered (a so-called "positive geometry", which represents the usual case), $K_I(a)$ is a monotonically increasing function of the crack length a (Eq. (5)). Since the second of the two inequalities of the system (6) requires the average (over Δ) SIF K_I to be larger than the fracture toughness K_{Ic}, it follows that $K_I(\Delta)$ is always

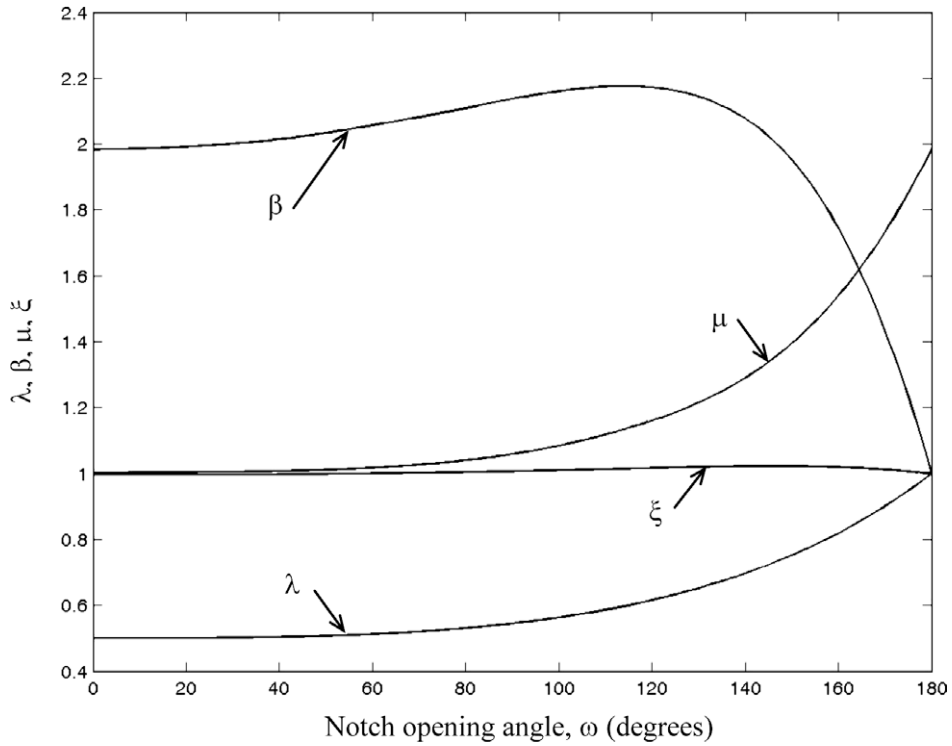

Fig. 2. λ-, β-, μ- and ξ-functions vs. notch opening angle ω.

larger than K_{Ic}. Hence, for the examined geometry, the crack stemming from a V-notch propagates always unstably.

3. Notch sensitivity and critical notch opening angle

Eq. (9) (or, equivalently, Eq. (10)) can be analyzed from two different points of view, i.e. either by varying α (i.e. s) and keeping ω fixed, or by varying ω and keeping α (i.e. s) fixed.

In the former case, the result is drawn in Fig. 3, where the relative strength is plotted vs. the dimensionless notch depth α for different ω values. It is evident that the minimum failure load is provided by the edge crack case only for $\alpha \to \infty$ ($s \to 0$), whereas it corresponds to the flat edge for $\alpha \to 0$ ($s \to \infty$). In the intermediate cases, the minimum failure load is provided by a V-notch of amplitude ω_c ranging from 0° up to 180° as α decreases from infinite to zero.

Also the envelope has been drawn in Fig. 3, i.e. the line that is tangent to all the diagrams plotted keeping ω fixed. It is clear that the envelope (thick black line) provides the minimum achievable by the relative failure stress for each relative notch depth α.

A further interesting consideration can be derived from Fig. 3. Let us consider the curves related to the extreme cases $\omega = 0°$ and $\omega = 180°$. They correspond to a failure described respectively by $K_I = K_{Ic}$ and $\sigma_f = \sigma_u$; they intersect each other at a relative notch depth $\alpha_0 = (1.12^2\pi)^{-1}$ corresponding to an edge crack of length:

$$e_0 = \frac{1}{\pi}\left(\frac{K_{Ic}}{1.12\sigma_u}\right)^2 \tag{11}$$

Observe that e_0 is a length characteristic of the material. Since the structural strength cannot exceed σ_u, a material is usually said to be insensitive to cracks shorter than e_0 (Carpinteri, 1997). However, from Fig. 3 it is evident there exist notches that are able to weaken the structures even if shorter than e_0. In other words, structures are more sensitive to notches than to cracks, although for large crack/notch depths a crack usually provides a stronger strength decrement with respect to a notch.

Now, let us consider the latter case, i.e. plot Eq. (10) by varying ω and keeping s fixed. The results are shown in Fig. 4: it is clear that there exists always a critical notch angle ω_c (corresponding to a minimum failure stress), whose position moves from 0° to 180° as the brittleness number s increases. Observe that: (i) the minimum is more pronounced for large s values, while it becomes almost imperceptible for small s; (ii) although curves referring to large s values may provide strengths higher than the material tensile strength (and are therefore unacceptable), the failure stress at the minimum is always lower than the material tensile strength.

The locus of the minima is represented in Fig. 4 by the thick line: the larger are the values of s (i.e. relatively ductile materials and/or small notch depths), the larger are the critical notch amplitude expected. On the contrary, for small s values (i.e. very brittle materials and/or large notch depths), the critical notch opening angle tends to vanish and the crack tends to become the most dangerous configuration.

Eventually, the determination of the critical notch angle may be formalized by deriving Eq. (9) with respect to ω and imposing the stationarity condition:

$$\frac{d(\sigma_f/\sigma_u)}{d\omega} = \alpha^{\lambda-1}\left(\lambda'\frac{\xi}{\beta}\ln\alpha + \frac{\xi'\beta - \xi\beta'}{\beta^2}\right) = 0 \tag{12}$$

where the prime denotes the derivative with respect to the notch opening angle ω. Hence the following relationship is obtained:

$$\alpha = \exp\left[\frac{1}{\lambda'}\left(\frac{\beta'}{\beta} - \frac{\xi'}{\xi}\right)\right]\Bigg|_{\omega=\omega_c} \tag{13}$$

By evaluating the derivatives λ', β' and ξ', the inverse of Eq. (13) is plotted in Fig. 5 and tabulated in Table 2. It is the relationship we were looking for, since it provides the value of the critical notch

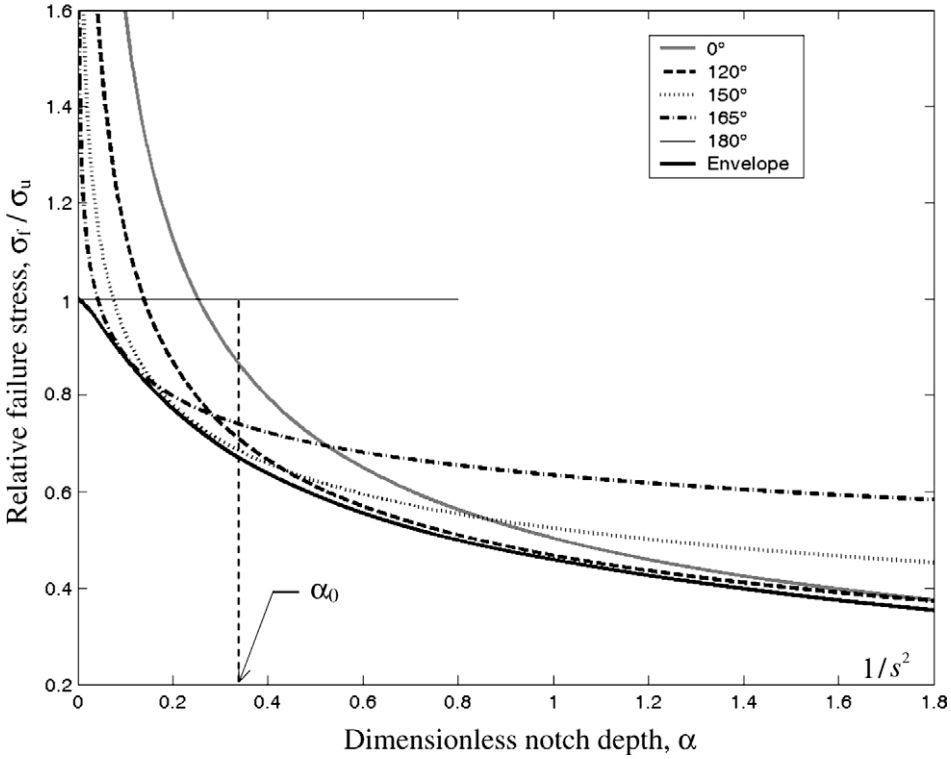

Fig. 3. Dimensionless failure load vs. dimensionless notch depth for $\omega = 0°$ (grey thick line), 120° (dashed line), 150° (dotted line), 165° (dot-dashed line) and 180° (thin line). The black thick line is the envelope of the other curves.

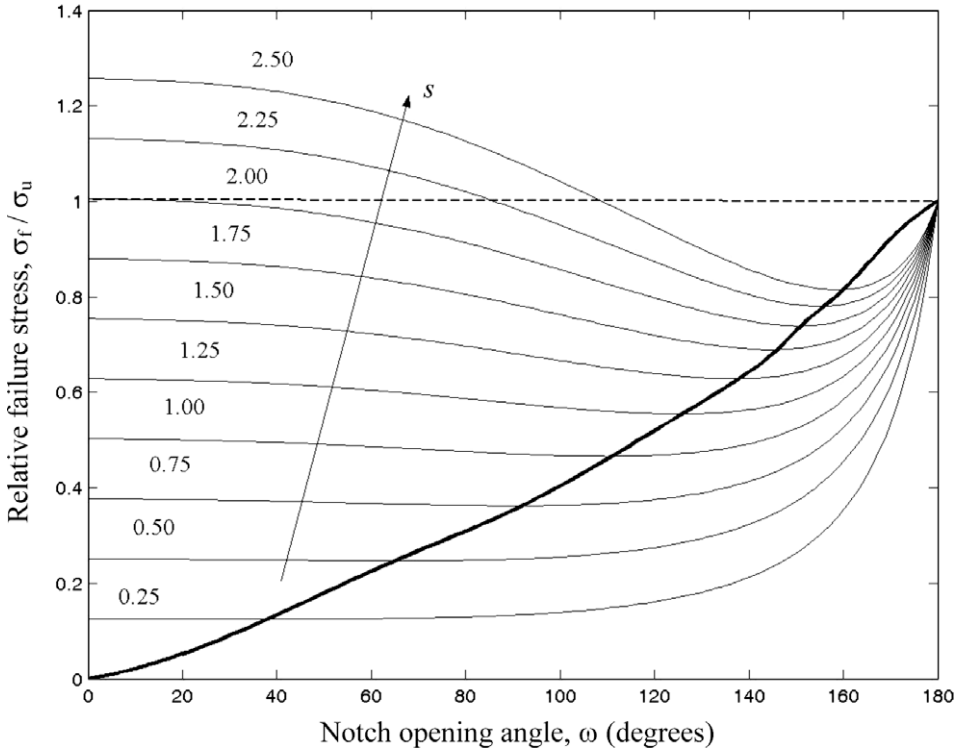

Fig. 4. Dimensionless failure load vs. opening angle ω for increasing values of the brittleness number s. The thick line represents the locus of the minima.

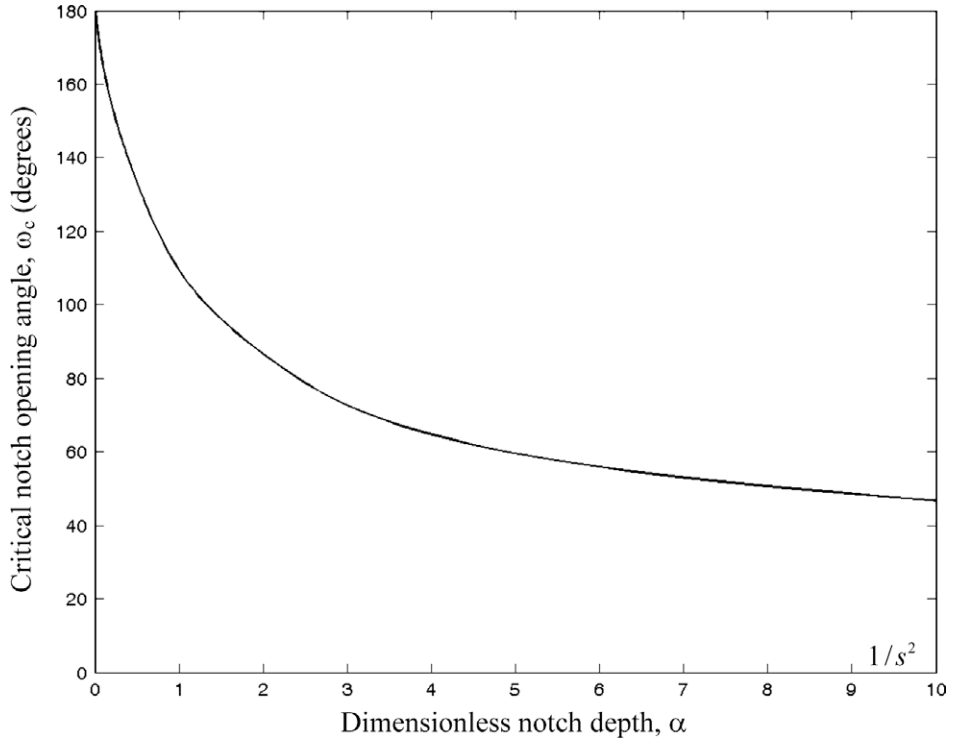

Fig. 5. Critical notch opening angle ω_c vs. dimensionless notch depth α.

opening angle ω_c for a given α (or s) value. Consistently with the previous analysis, ω_c depends through s both on the material and the geometry. It is evident that the crack is the most dangerous V-notch ($\omega_c = 0$) only for extremely large notches and/or very brittle materials.

4. Discussion of the results

In the authors' opinion, the present analysis catches the basic features of the problem under examination, i.e. the presence of a non-zero notch opening angle providing the lowest failure load.

Table 2
Critical notch opening angle ω_c vs. dimensionless notch depth α.

α	ω_c (°)	α	ω_c (°)
0	180.0	6	56.1
0.25	150.5	7	53.1
0.50	133.4	8	50.6
0.75	119.9	9	48.5
1	109.7	10	46.8
2	86.9	12.5	43.2
3	72.7	15	40.2
4	64.4	17.5	37.7
5	59.7	20	35.6

However, it should be noted that the analysis carried out is mainly theoretical for two reasons: (i) for very short notches (i.e. small α/large s) the failure criterion represented by Eq. (3) does not hold true, analogously to what happens to LEFM (i.e. $K_I = K_{Ic}$) for short cracks; (ii) it refers to a semi-infinite plate.

The first remark implies that the plot in Fig. 5 may be not precise for small α. This drawback can be overcome by using the actual stress and SIF values instead of the asymptotic fields (Eqs. (1) and (5)), as done in (Cornetti et al., 2009) for shallow V-notches with opening angle equal to 120°. Nevertheless, the plot in Fig. 5 shows that the critical angle tends slowly to zero as the notch depth and/or the material brittleness increases (large α). Hence, the critical notch amplitude is expected to be larger than 0° also for full-sized notches, for which α is usually much larger than unity. Although a direct comparison is not possible due to the infinite geometry considered in the present analysis, this finding is in agreement with experimental data available in the literature and cited in Section 1.

The second remark can be overcome by introducing suitable shape functions. When passing from infinite (Fig. 1a) to finite (Fig. 1b) geometries, dimensional analysis arguments show that Eq. (2) has to be replaced by:

$$K_I^* = \sigma h^{1-\lambda} f(e/h, l/h, \omega) \tag{14}$$

where h is the specimen height, l its length and f is the shape function, depending now not only on the amplitude but also on the relative notch depth and the slenderness ratio. By means of Eqs. (3), (4) and (14), the failure stress becomes:

$$\frac{\sigma_f}{\sigma_u} = \frac{\xi(\omega)}{f(e/h, l/h, \omega)} s^{2(1-\lambda)} \tag{15}$$

where now the brittleness number has the usual expression $s = K_{Ic}/(\sigma_u\sqrt{h})$. From Eq. (15) it is clear that the failure stress as well as the possible presence of a minimum depends on the fracture criterion adopted (through ξ), on the specimen shape (through f), on the notch opening angle (through f, ξ and λ) and on the material and the specimen absolute size (through s).

The comparison between experimental data and theoretical predictions based on different failure criteria requires to compute numerically the shape function for each geometry and is beyond the scope of the present paper. Here we just want to say that some comparisons can be found in the recent papers (Carpinteri et al., 2008, 2009), where the numerical analyses highlighted, through Eq. (15), the presence of a minimum also in finite geometries. Furthermore, for what concerns the detection of the minimum in the experiments, preliminary results seem to indicate that the FFM coupled criterion (Cornetti et al., 2006) and the strain energy density based criterion (Lazzarin and Zambardi, 2001; Lazzarin et al., 2009) work more properly, the latter one providing the most pronounced minimum (although not evident in the K_{Ic}^* vs ω plots of (Lazzarin and Zambardi, 2001), whose shape depends on the physical dimension chosen and turns out to be monotonically increasing). On the other hand, applications of the cohesive crack model (Gómez and Elices, 2003), of the FFM criterion by Leguillon (2002) and of the average stress criterion (Seweryn, 1994) tends to provide monotonically increasing failure loads.

Eventually, we want to stress that all the analysis herein provided is under the hypothesis of the sharpness of the V-notch. In order to make comparisons with experimental data, beyond finite sizes, it can be necessary to consider explicitly the presence of a notch root radius following, e.g., the procedure outlined in (Atzori and Lazzarin, 2001; Leguillon and Yosibash, 2003; Pugno et al., 2005). Moreover, one should be aware that the present model is two-dimensional, whereas real structures are always three-dimensional; recent studies (Berto et al., 2004; Kotousov, 2007; Kotousov et al., 2009) have shown that, even in the geometry analyzed, there can be three-dimensional effects influencing the failure stress.

5. Conclusions

The problem of determining the most severe notch opening angle (i.e. the angle providing the minimum failure load) in a semi-infinite V-notched slab under remote tension has been addressed in the present paper. Under the assumptions of notch sharpness and structural brittleness, it was found that, according to the widely accepted LEFM-like criterion $K_I^* = K_{Ic}^*$ (Eq. (3)) and contrarily to what expected, the edge crack is not the most dangerous configuration and that the critical amplitude depends both on notch depth and material properties through the brittleness number. This important theoretical finding is in agreement with most of the experimental data available in the literature.

References

Atzori, B., Lazzarin, P., 2001. Notch sensitivity and defect sensitivity under fatigue loading: two sides of the same medal. Int. J. Fract. 107, L3–L8.

Berto, F., Lazzarin, P., Wang, C.H., 2004. Three-dimensional linear elastic distributions of stress and strain energy density ahead of V-shaped notches in plates of arbitrary thickness. Int. J. Fract. 127, 265–282.

Carpinteri, A., 1981a. Size effect in fracture toughness testing: a dimensional analysis approach. In: Sih, G.C., Mirabile, M. (Eds.), Analytical and Experimental Fracture Mechanics (Proceedings of the International Conference on Analytical and Experimental Fracture Mechanics, Roma, Italy, 1980). Sijthoff & Noordhoff, Alphen aan den Rijn, pp. 785–797.

Carpinteri, A., 1981b. Static and energetic fracture parameters for rocks and concrete. Mater. Struct. 14, 151–162.

Carpinteri, A., 1982. Notch sensitivity in fracture testing of aggregative materials. Eng. Fract. Mech. 16, 467–481.

Carpinteri, A., 1987. Stress-singularity and generalized fracture toughness at the vertex of re-entrant corners. Eng. Fract. Mech. 26, 143–155.

Carpinteri, A., 1997. Structural Mechanics: A Unified Approach. Chapman & Hall, London.

Carpinteri, A., Pugno, N., 2005. Fracture instability and limit strength conditions in structures with re-entrant corners. Eng. Fract. Mech. 72, 1254–1267.

Carpinteri, A., Cornetti, P., Pugno, N., Sapora, A., Taylor, D., 2008. A finite fracture mechanics approach to structures with sharp V-notches. Eng. Fract. Mech. 75, 1736–1752.

Carpinteri, A., Cornetti, P., Pugno, N., Sapora, A., Taylor, D., 2009. Generalized fracture toughness for specimens with re-entrant corners: experiments vs. theoretical predictions. Struct. Eng. Mech. 32, 609–620.

Cornetti, P., Pugno, N., Carpinteri, A., Taylor, D., 2006. Finite fracture mechanics: a coupled stress and energy failure criterion. Eng. Fract. Mech. 73, 2021–2033.

Cornetti, P., Taylor, D., Carpinteri, A., 2009. An asymptotic matching approach to shallow-notched structural elements. Eng. Fract. Mech.. doi:10.1016/j.engfracmech.2009.04.013.

Dunn, M., Suwito, W., Cunnigham, S., 1997. Stress intensities at notch singularities. Eng. Fract. Mech. 57, 417–430.

Dunn, M.L., Suwito, W., Cunningham, S., 1997. Fracture initiation at sharp notches: correlation using critical stress intensities. Int. J. Solids Struct. 34, 3873–3883.

Gómez, F.J., Elices, M., 2003. A fracture criterion for sharp V-notched samples. Int. J. Fract. 123, 163–175.

Gómez, F.J., Elices, M., 2003. Fracture of components with V-shaped notches. Eng. Fract. Mech. 70, 1913–1927.

Grenestedt, J.L., Hallström, S., Kuttenkeuler, J., 1996. On cracks emanating from wedges in expanded PVC foam. Eng. Fract. Mech. 54, 445–456.

Hasebe, N., Iida, J., 1978. A crack originating from a triangular notch on a rim of a semi-infinite plate. Eng. Fract. Mech. 10, 773–782.

Kotousov, A., 2007. Fracture in plates of finite thickness. Int. J. Solids Struct. 44, 8259–8273.

Kotousov, A.G., Harding, S., Lazzarin P., 2009. On plate thickness effect in plane problems of elasticity. In: Proceedings of the Conference "Crack Paths", Vicenza, Italy, 23–25 September, 2009.

Lazzarin, P., Zambardi, R., 2001. A finite-volume-energy based approach to predict the static and fatigue behavior of components with sharp v-shaped notches. Int. J. Fract. 112, 275–298.

Lazzarin, P., Berto, F., Elices, M., Gómez, J., 2009. Brittle failures from U- and V-notches in mode I and mixed, I + II, mode: a synthesis based on the strain energy density averaged on finite-size volumes. Fatigue Fract. Eng. Mater. Struct. 32, 671–684.

Leguillon, D., 2002. Strength or toughness? A criterion for crack onset at a notch. Eur. J. Mech. A/Solids 21, 61–72.

Leguillon, D., Yosibash, Z., 2003. Crack onset at a v-notch. Influence of the notch tip radius. Int. J. Fract. 122, 1–21.

Livieri, P., Tovo, R., 2009. The use of the J_V parameter in welded joints: stress analysis and fatigue assessment. Int. J. Fatigue 31, 153–163.

Philipps, A.G., Karuppanan, S., Churchman, C.M., Hills, D.A., 2008. Crack tip stress intensity factors for a crack emanating from a sharp notch. Eng. Fract. Mech. 75, 5134–5139.

Pugno, N., Peng, B., Espinosa, H.D., 2005. Predictions of strength in MEMS components with defects – a novel experimental-theoretical approach. Int. J. Solids Struct. 42, 647–661.

Seweryn, A., 1994. Brittle fracture criterion for structures with sharp notches. Eng. Fract. Mech. 47, 673–681.

Sih, G.C., Ho, J.W., 1991. Sharp notch fracture strength characterized by critical energy density. Theor. Appl. Fract. Mec. 16, 179–214.

Strandberg, M., 2002. Fracture at V-notches with contained plasticity. Eng. Fract. Mech. 69, 403–415.

Williams, M.L., 1952. Stress singularities resulting from various boundary conditions in angular corners of plate in extension. J. Appl. Mech. 19, 526–528.